A comparison of cement and Guar Gum stabilisation of Oxford clay under controlled wetting and drying cycles.

applied sciences

MDPI

Article

A Comparison of Cement and Guar Gum Stabilisation of Oxford Clay Under Controlled Wetting and Drying Cycles

Kanishka Sauis Turrakheil, Syed Samran Ali Shah and Muhammad Naveed *

School of Computing and Engineering, University of West London, London W5 5RF, UK; kanishka.turrakheil@uwl.ac.uk (K.S.T.); syed.shah@uwl.ac.uk (S.S.A.S.)
* Correspondence: muhammad.naveed@uwl.ac.uk

Abstract: Climate-induced wetting and drying (WD) cycles significantly affect the long-term performance of geotechnical structures. This study explores expansive Oxford clay's mechanical and volumetric responses stabilised with ordinary Portland cement (OPC) and guar gum (GG) under repeated WD cycles. We prepared 108 samples in total—36 untreated, 36 treated with OPC, and 36 treated with GG. These samples were compacted to 90% of their maximum dry density and subjected to 1, 5, 10, and 15 WD cycles, with nine samples for each treatment at each cycle. During the WD cycles, we monitored volumetric strain and moisture content. Mechanical performance was assessed through unconsolidated undrained triaxial tests conducted at matric suctions of −1500 kPa, −33 kPa, and under saturated conditions. We evaluated the undrained shear strength (S_u), secant modulus of elasticity (E_{50}), and modulus of toughness (U_t). The results showed that OPC-treated samples consistently exhibited the highest S_u at −1500 kPa across all WD cycles, followed by untreated and GG-treated samples. At −33 kPa, OPC-treated samples again outperformed the others in S_u, while GG-treated samples performed better than the untreated ones. Under saturated conditions, GG-treated samples displayed a similar S_u to OPC-treated samples, significantly higher than untreated samples. Energy absorption capacity, measured through U_t, peaked for OPC-treated samples at −1500 kPa but favoured GG treatment at −33 kPa and under saturation. X-ray computed tomography (CT) revealed severe degradation in untreated samples, characterised by extensive cracking, minor cracking in OPC-treated samples, and minimal damage in GG-treated samples. This highlights the superior resilience of guar gum to wetting–drying cycles. These findings underscore the potential of guar gum as a sustainable alternative to cement for enhancing the WD resilience of expansive soils, particularly under low-suction or saturated conditions.

Keywords: Oxford clay; wetting and drying cycles; cement and guar gum stabilisation; undrained shear strength; modulus of elasticity and modulus of toughness

Academic Editor: Eduardo Garzon

Received: 23 May 2025
Revised: 16 June 2025
Accepted: 17 June 2025
Published: 19 June 2025

Citation: Turrakheil, K.S.; Shah, S.S.A.; Naveed, M. A Comparison of Cement and Guar Gum Stabilisation of Oxford Clay Under Controlled Wetting and Drying Cycles. *Appl. Sci.* **2025**, *15*, 6913. https://doi.org/10.3390/app15126913

1. Introduction

Climate change poses serious risks to geotechnical infrastructure's long-term performance and stability, including roads, embankments, landfill covers, and flood defences. Traditionally, these systems were designed based on static climatic and hydrological conditions. However, the increasing frequency and intensity of extreme weather events, such as heavy rainfall, prolonged droughts, heatwaves, and rising sea levels—driven by human-induced climate change [1]—undermine these assumptions. Consequently, many earth structures are now subjected to environmental stresses that surpass their original design capacities. One significant effect of changing climatic conditions is the alteration of soil

moisture regimes. Fluctuations in moisture content due to extreme precipitation or extended dry periods can substantially impact the mechanical behaviour of soils, reducing shear strength, stiffness, and structural integrity [2–4]. Clayey soils, common in many regions, are particularly vulnerable to environmental processes that change their hydro-mechanical properties. Among these processes, cyclic wetting and drying (WD) has become a major mechanism of soil degradation, especially in semi-arid and tropical climates, where seasonal moisture changes frequently occur [5,6]. These wetting and drying cycles cause repetitive swelling and shrinkage, resulting in cumulative damage such as fissuring, disaggregation, microstructural changes, and declines in strength and stiffness [7–9]. At the microstructural level, WD cycles induce alterations in pore structure, particle orientation, and fabric connectivity, which ultimately affect permeability and collapse potential [7,10,11]. Furthermore, physico-chemical interactions, such as cation exchange, mineral dissolution, and re-precipitation, further exacerbate degradation [12]. Despite increased awareness of these processes, our understanding of the long-term mechanical evolution of soils subjected to repeated WD cycles is still limited, with most studies focusing on a limited number of WD cycles [13,14].

Cement stabilisation is a widely accepted technique that decreases plasticity, limits swelling potential, and significantly enhances shear strength properties [15,16]. Even at low dosages, cement improves unconfined compressive strength (UCS) and California Bearing Ratio (CBR) by forming cementitious hydration products that bind soil particles and reduce moisture susceptibility [17,18]. Long-term field evaluations, such as a 45-year study conducted in Oklahoma, have shown that cement-treated clays maintain improved strength and plasticity long after treatment [19]. This durability is primarily due to the formation of sturdy pozzolanic bonds that resist environmental degradation [17,20,21]. However, the ecological impact of cement production, known for high CO_2 emissions and increased soil alkalinity, has prompted a search for more sustainable alternatives [22]. Among these alternatives, biopolymers such as guar gum have gained attention for their environmentally friendly properties and effective soil improvement capabilities. Derived from the guar bean, guar gum is a galactomannan polysaccharide that forms a viscous gel upon hydration, binding soil particles into a flexible yet robust matrix. This matrix minimises desiccation cracking, limits swelling during wetting, enhances shear strength, and reduces the permeability of treated soils [23–25]. Additionally, guar gum treatments have been shown to raise expansive clays' plastic and shrinkage limits, thereby improving their resistance to volumetric changes across a broader moisture range [26]. Unlike cement, biopolymer treatments do not significantly alter soil pH or introduce long-term chemical changes, making them more compatible with sensitive ecological contexts. Experimental studies on guar gum have reported significant improvements in UCS, CBR, and shear strength parameters, like cohesion and internal friction angle [23,24]. The stabilisation mechanism is predominantly physical, creating hydrogel networks that coat and interconnect soil particles, alleviating moisture-induced strains and enhancing aggregate stability. Notably, studies have shown up to 50% reductions in swell index and swell pressure in expansive clays treated with guar gum and marked decreases in shrinkage cracking [24,25].

Building on previous research, this study aims to compare the long-term durability of cement and guar gum-stabilised Oxford clay under repeated wetting and drying (WD) cycles. The assessment will include (a) the behaviour of volumetric changes, focusing on monitoring swelling and shrinkage strains throughout successive WD cycles; (b) the mechanical response, which includes undrained shear strength, modulus of elasticity, and toughness, evaluated through triaxial testing under multiple WD cycles and varying moisture states; and (c) a cost–carbon analysis comparing the economic and environmental feasibility of stabilising 1 m^3 of soil using each additive.

2. Materials and Methods

2.1. Materials

This study utilised Oxford clay sourced from Eynsham, Oxfordshire, UK, with approximate coordinates of 51°46′55″ N and 1°23′05″ W. Oxford clay is a Jurassic-aged, highly plastic clay known for its significant shrink–swell behaviour. Samples were collected from depths ranging from 0.25 to 3.0 m below ground level, within a clay stratum beneath superficial sand and gravel deposits. Groundwater was found at depths between 0.9 and 2.93 m, indicating that the clay typically remains relatively moist. In its natural condition, the clay is grey and silty, with occasional shell fragments and a slight organic odour. Initial laboratory characterisation of the air-dried and pulverised soil confirmed its high plasticity. The particle size distribution, determined through combined sieve and hydrometer analysis, was approximately 60% clay, 37% silt, and 3% sand. The Atterberg limit tests yielded a liquid limit (LL) of 53% and a plastic limit (PL) of 22%, resulting in a plasticity index (PI) of 31. Based on these indices, the soil is classified as a high-plasticity clay (CH) under the Unified Soil Classification System (USCS) and as group A-7-6 according to the AASHTO classification. The natural pH of the clay ranged from 7.4 to 8.4. Modified Proctor compaction tests determined an optimum moisture content (OMC) of approximately 12% and a maximum dry density (MDD) of 1.80 g/cm^3. The high plasticity index (PI) and the moderate OMC indicate a medium-to-high swell potential. Given these properties, Oxford clay is considered a suitable candidate for investigating the effectiveness of stabilisation under moisture cycling.

Two stabilising agents were used: ordinary Portland cement (OPC) and guar gum (GG). OPC was added at 6% by dry weight of soil, a dosage commonly used for subgrade stabilisation to enhance strength and reduce plasticity. This percentage aligns with field applications, such as in the stabilisation of the Oklahoma US-62 Highway [19], and falls within the recommended range of 3–8% [27]. The effectiveness of cement arises from the hydration of tricalcium silicate (C_3S) and dicalcium silicate (C_2S), which produce calcium silicate hydrate (C–S–H) gel and calcium hydroxide [$Ca(OH)_2$]—the primary agents for binding and soil improvement. Guar gum, a natural biopolymer, was used at 1% by dry weight of soil. The guar gum used was a commercially available food-grade powder (greater than 99% purity), with a manufacturer-reported average molecular weight of 1.0 million Da. It is derived from the endosperm of guar beans (Cyamopsis tetragonoloba) and forms a highly viscous gel when hydrated [28]. This dosage is within the optimal range (0.5–2%) reported in the literature for clayey soils, beyond which strength improvements tend to plateau [28]. Both stabilisers were applied in dry-powder form and thoroughly mixed with the pulverised soil to ensure uniform distribution before adding water.

2.2. Preparation of Soil Samples

Bulk soil collected from the site was initially air-dried and then oven-dried at 105 °C for at least 24 h, following the guidelines outlined in BS 1377-1:2016 [29]. After drying, the soil was crushed and sieved through a 2 mm sieve to break apart clods and remove gravel-sized particles. This resulted in a uniform fine-grained matrix suitable for laboratory testing. Stabilising agents—either 6% ordinary Portland cement (OPC) or 1% guar gum (GG) by dry weight of soil—were carefully mixed with the prepared soil. This mixing was performed manually and supplemented with a mechanical mixer to ensure uniformity. Once the dry mixing was complete, water was incrementally sprayed onto the mixture and thoroughly blended until the target moisture content was reached. All samples were compacted at an approximately optimal moisture content (OMC) of 12% and 90% of the modified Proctor maximum dry density (MDD). Specimen preparation involved static compaction of the moist soil mixture within cylindrical moulds to create samples measuring

50 mm in diameter and 100 mm in height (height-to-diameter ratio of 2:1), which minimised boundary effects during triaxial testing. Each specimen was compacted in four layers to reduce air entrapment and promote uniform density. One hundred and eight samples were prepared and evenly divided into three groups: untreated, cement-stabilised, and guar gum-stabilised, with 36 samples in each group. Each group was further subdivided based on the number of wetting–drying (WD) cycles: 1, 5, 10, and 15, with nine replicates for each condition (Figure 1). The 1-cycle group served as control samples, representing the initial condition—they were compacted, cured, and reconstituted without undergoing cyclic moisture changes, thereby isolating the immediate effects of stabilisation without any environmental degradation. After compaction, all samples were cured under controlled laboratory conditions for 7 days at 25 ± 2 °C, wrapped in sealed plastic to prevent moisture loss. This curing period allowed for initial cement hydration and guar gum gel formation, while maintaining the same conditions for untreated samples to ensure consistency in the experiment. No additional water was added during the curing period, and all samples were handled carefully to prevent premature drying or shrinkage cracking, especially in the cement-treated samples.

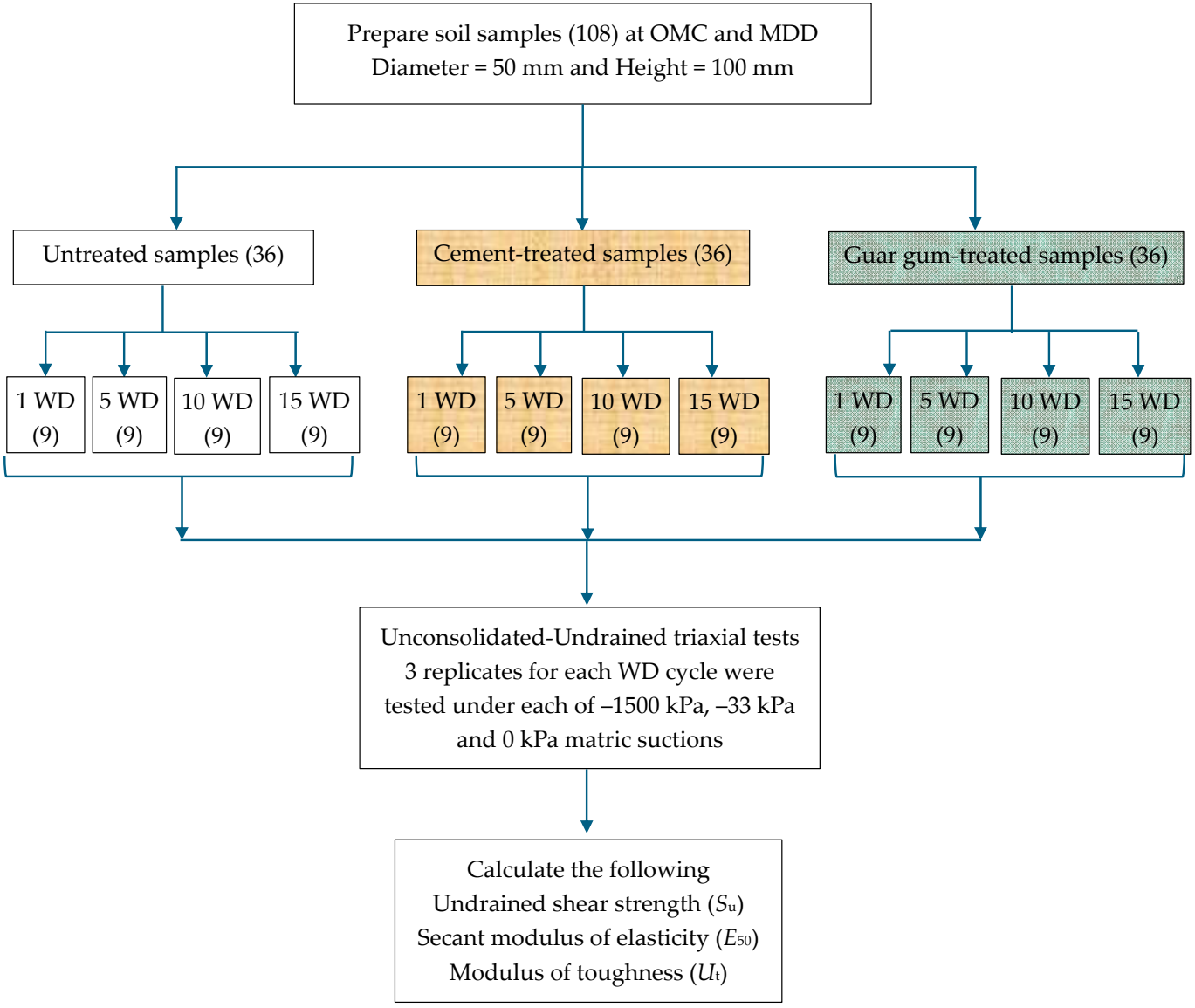

Figure 1. Flowchart of the study. OMC = optimum moisture content, MDD = maximum dry density, WD = wetting–drying cycles.

Following curing, the soil samples underwent the designated wetting–drying (WD) cycles (Figure 1). One WD cycle was defined as one complete sequence of wetting followed by drying. Wetting was performed by submerging the base of each specimen in water, allowing capillary rise until saturation was reached. The duration of the wetting phase varied among samples and treatments, although it remained fairly consistent within each treatment group. Due to changes in permeability and pore structure, later cycles required longer wetting times, especially for treated samples. Drying phases were carried out in a humidity-controlled chamber or desiccation apparatus designed to induce matric suction of approximately −1500 kPa, corresponding to moisture contents near the plastic limit or OMC of the clay. Each specimen was subjected to its assigned number of WD cycles (1, 5, 10, or 15), with particular care taken to avoid mechanical damage, especially during handling in the softened, saturated state.

2.3. Measurement of Volumetric Strain

Following each wetting–drying (WD) cycle, volume measurements were conducted on the soil samples to analyse their volumetric behaviour over successive cycles. Measurements were performed using a high-precision electronic Vernier calliper with an accuracy of ±0.005 mm. For each specimen, the height (h_1, h_2, and h_3) and diameter (d_1, d_2, and d_3) were recorded at three equally spaced points along the specimen's surface to ensure representative data.

Measurements were performed with utmost care and minimal handling to minimise disturbance, particularly in samples with reduced structural integrity due to moisture after saturation. The average values of the height and diameter measurements were used to compute the specimen volume and the corresponding volumetric strain (ε_v) for each WD cycle.

The volumetric strain was calculated using the equation below.

$$\boldsymbol{\varepsilon_v = \frac{V_N - V_0}{V_0} \times 100} \quad (1)$$

where V_0 represents the initial volume of the compacted specimen, and V_N denotes the volume after N WD cycles. A positive ε_v value indicates swelling, while a negative value corresponds to shrinkage.

2.4. Unconsolidated–Undrained Triaxial Testing and Analysis

Unconsolidated–undrained (UU) triaxial compression tests were conducted in accordance with BS 1377: Part 7 (1990) [30] to evaluate the shear strength characteristics of the treated and untreated soil samples. All samples were tested at the end of their designated wetting–drying (WD) cycles. The samples were placed in a triaxial chamber and subjected to a constant confining pressure (cell pressure) of 50 kPa. Axial loading was applied under undrained conditions, and the test was continued until either failure occurred (indicated by a peak in deviator stress) or an axial strain of 20% was reached. The tests in triplicate were conducted at three moisture states (Figure 1).

- −1500 kPa matric suction: This represents a dry-season or post-compaction condition in which matric suction contributes to higher strength.
- −33 kPa matric suction: Samples were first fully saturated and then allowed to dry partially. This condition simulates field capacity, such as a few days after the rainfall.
- Full saturation: Achieved through prolonged soaking to eliminate matric suction, this represents the worst-case scenario, such as heavy rainfall or flooding, when strength is lowest due to the absence of suction.

Each sample was tested at room temperature (~20 °C), and axial loading was applied using a compression machine at a constant strain rate of 0.1 mm/min. For soft or fully saturated samples, a slower rate of 0.01 mm/min was used to reduce the risk of sudden failure and to ensure accurate observation of stress–strain behaviour. The applied strain rate was selected to maintain undrained conditions by preventing significant pore-pressure dissipation during the test. From each test, the deviator stress–axial strain response was recorded. The undrained shear strength (S_u) was calculated as half of the peak deviator stress at failure. The undrained secant modulus of elasticity (E_{50}) was calculated using Equation (2), and the modulus of toughness (U_t) was calculated using Equation (3).

$$E_{50} = \frac{0.5 \times \Delta\sigma_{max}}{\varepsilon_{50}} \quad (2)$$

$$U_t = \int_0^{\varepsilon_{failure}} \Delta\sigma(\varepsilon)d\varepsilon \quad (3)$$

where $\Delta\sigma_{max}$ is the maximum deviatoric stress, ε_{50} is the strain corresponding to 50% of the maximum deviatoric stress, ε is the strain, and $\Delta\sigma$ is the deviatoric stress.

After testing, samples were oven-dried to determine the actual moisture content. Visual observations of each specimen's failure mode (e.g., bulging and shear plane development) were also made to assess ductility and brittleness qualitatively.

2.5. X-Ray CT Scanning and Visualisation

X-ray computed tomography (CT) scans were conducted on six soil samples—three after one wetting–drying (WD) cycle and three after ten WD cycles. Each treatment type (untreated, cement-treated, and guar gum-treated) was represented by one specimen per WD condition. Before scanning, all samples were equilibrated at a matric suction of −1500 kPa, using a pressure plate apparatus. Scanning was performed using a Nikon X-Trek XTH225ST system (Nikon, Minato City, Japan), operating at a maximum accelerating voltage of 195 kV and a current of 105 mA. A 0.5 mm copper filter was applied to the X-ray beam to reduce beam-hardening effects. Each scan acquired 1800 projections over a full 360° rotation, with a two-second exposure per projection. The resulting data were reconstructed using Nikon's proprietary filtered back-projection algorithm, yielding a voxel resolution of 50 µm. Radiographs were reconstructed in 32-bit format to preserve the full dynamic range of the grayscale histogram. Image processing and analysis were performed using ImageJ version 1.54 [31].

3. Results

3.1. Moisture Dynamics and Volumetric Behaviour Under WD Cycles

In the first and second wetting cycles, untreated samples reached saturation moisture contents of 26% and 27%, respectively, accompanied by swelling strains of approximately 14%. In subsequent cycles, the saturated moisture contents and swelling magnitudes diminished, stabilising within 20–25% and 8 to 10%, respectively. Drying was carried out to a target matric suction of −1500 kPa, resulting in 12 ± 1% residual moisture contents. The associated shrinkage strains varied between −2% and −7%. This pronounced volumetric response underscores the high susceptibility of the untreated expansive soil to structural degradation under cyclic hydric loading (Figure 2).

In contrast, cement-treated samples exhibited markedly different behaviour. During the initial wetting phase, these samples attained a saturation moisture content of 34% and exhibited swelling strains of 22%, significantly exceeding those of their untreated counterparts (Figures 2 and 3). Following drying to −1500 kPa, the samples retained a residual expansion of approximately 15%, even though the moisture content reverted to

the initial optimum moisture content (OMC). Over the 15 wetting–drying (WD) cycles, the swelling strain under saturated conditions progressively increased, reaching up to 30%. However, the post-drying residual swelling stabilised at approximately 15%. Notably, the saturation moisture content increased with each cycle, eventually peaking at 43% (Figure 2).

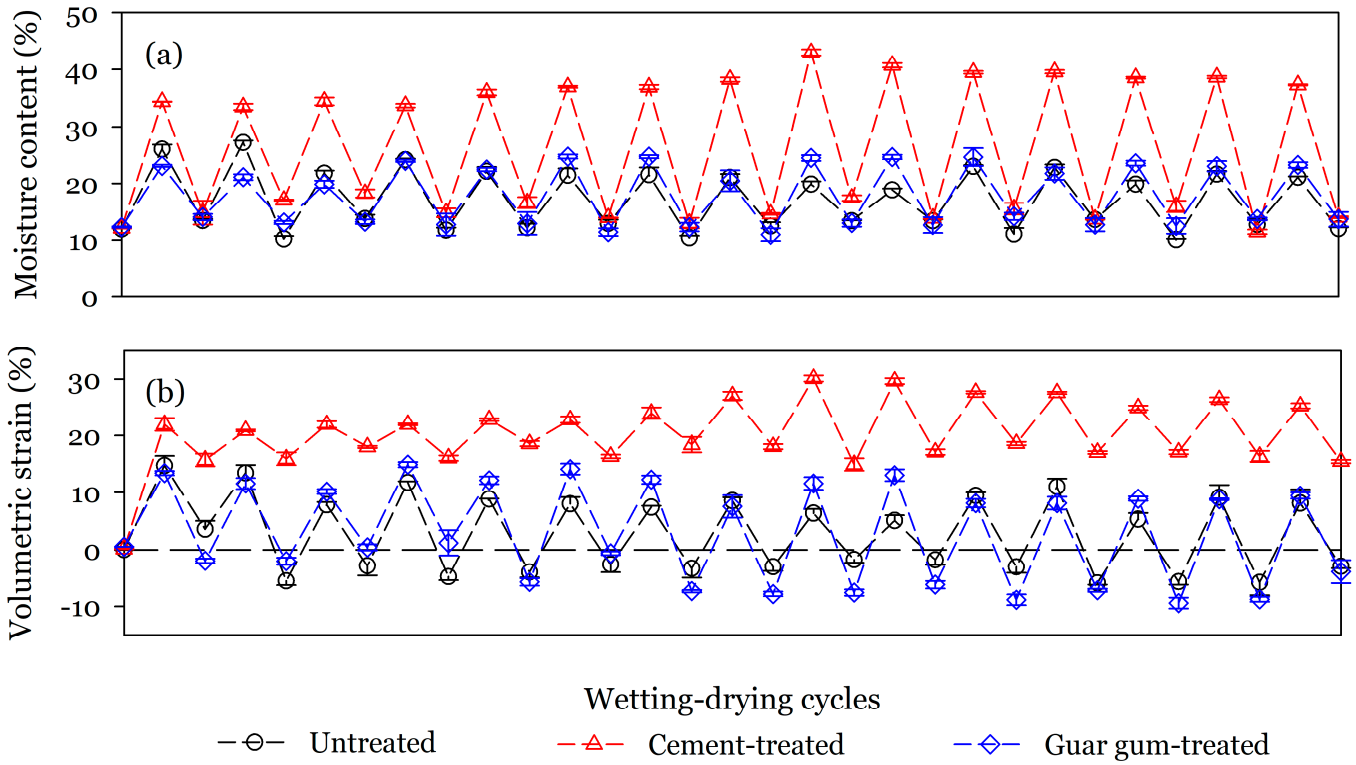

Figure 2. (**a**) Variation in moisture content between saturation (target wetting) and a matric suction of −1500 kPa (target drying) with wetting–drying cycles and (**b**) variation in volumetric strain with wetting–drying cycles for cement-treated, guar gum-treated, and untreated soil.

The volumetric response of guar gum-treated samples was similar to that of the untreated soils. Across the WD cycles, swelling strains ranged between 10% and 13%, comparable to the untreated soil (~12%). Drying-induced shrinkage strains varied from −1 to −6%, mirroring the untreated response in magnitude. Despite the similarity in strain amplitudes, the guar gum treatment appreciably altered the water-infiltration behaviour. Guar gum-treated samples required six days to reach full saturation, in contrast to four days for the untreated counterparts. The saturation moisture contents in the first two cycles were 23% and 21%, respectively, lower than those of the untreated samples. In later cycles, saturation levels remained within the 20–25% range, similar to the untreated samples (Figure 2). Although the overall swelling–shrinkage amplitude remained unchanged, visual inspection revealed that guar gum-treated samples exhibited enhanced structural integrity. Desiccation cracking was severely reduced, with finer and more superficial cracks compared to the extensive cracking observed in untreated samples by cycle 10. The guar gum matrix likely functioned as a biopolymeric binder, preserving the columnar structure and limiting crack propagation [26,32].

3.2. Stress–Strain Behaviour at −1500 kPa Matric Suction

All tested soils exhibited relatively stiff behaviour at −1500 kPa matric suction, representing a near-dry strength condition. The deviator stress–axial strain responses (average for three samples) for untreated, cement-treated, and guar gum-treated samples tested at −1500 kPa matric suction following 1, 5, 10, and 15 wetting–drying (WD) cycles are pre-

sented in Figure 4. The corresponding moisture contents of the soil samples at −1500 kPa matric suction are given in Appendix A. Regardless of treatment type, all samples demonstrated strain-softening behaviour. Among the treatments, cement-treated samples consistently achieved the highest undrained shear strength (S_u), followed by untreated soils. At the same time, guar gum-treated samples exhibited the lowest S_u across all WD cycles. A progressive reduction in S_u was observed with increasing WD cycles for all treatment conditions (Figure 5a).

Figure 3. Comparison of volume change in samples treated with cement (**left**) and guar gum (**right**) at −1500 kPa of matric suction. The cement-treated specimen shows significant volume increase and cracking, whereas the guar gum-treated specimen exhibits minimal cracking and more stable volume.

Across all wetting–drying (WD) cycles, the secant modulus of elasticity (E_{50}) was the highest in untreated soil. In contrast, the guar gum- and cement-treated soils exhibited comparable but lower E_{50} values (Figure 5b). In comparison, the modulus of toughness consistently ranked highest in the cement-treated soil, followed by the guar gum-treated soil, with the untreated soil showing the lowest values throughout the WD cycles (Figure 5c).

3.3. Stress–Strain Behaviour at −33 kPa Matric Suction

Figure 6 presents the stress–strain responses (average of three samples) of untreated, cement-treated, and guar gum-treated soils assessed at −33 kPa matric suction following exposure to 1, 5, 10, and 15 wetting–drying (WD) cycles. The corresponding moisture contents are given in Appendix A. Unlike the untreated and guar gum-treated soils, the cement-treated samples consistently exhibited strain-softening behaviour, demonstrating pronounced strain-hardening characteristics across all WD cycles (Figure 6).

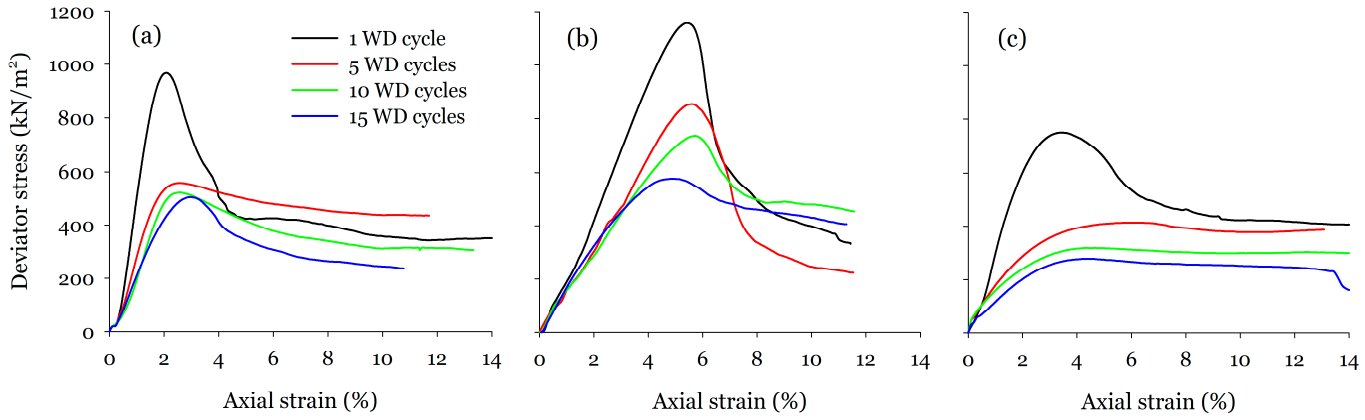

Figure 4. Deviator stress is plotted as a function of axial strain (average for three samples) measured at the matric suction of −1500 kPa for (**a**) untreated soil, (**b**) cement-treated soil, and (**c**) guar gum-treated soil for 1, 5, 10, and 15 wetting–drying cycles.

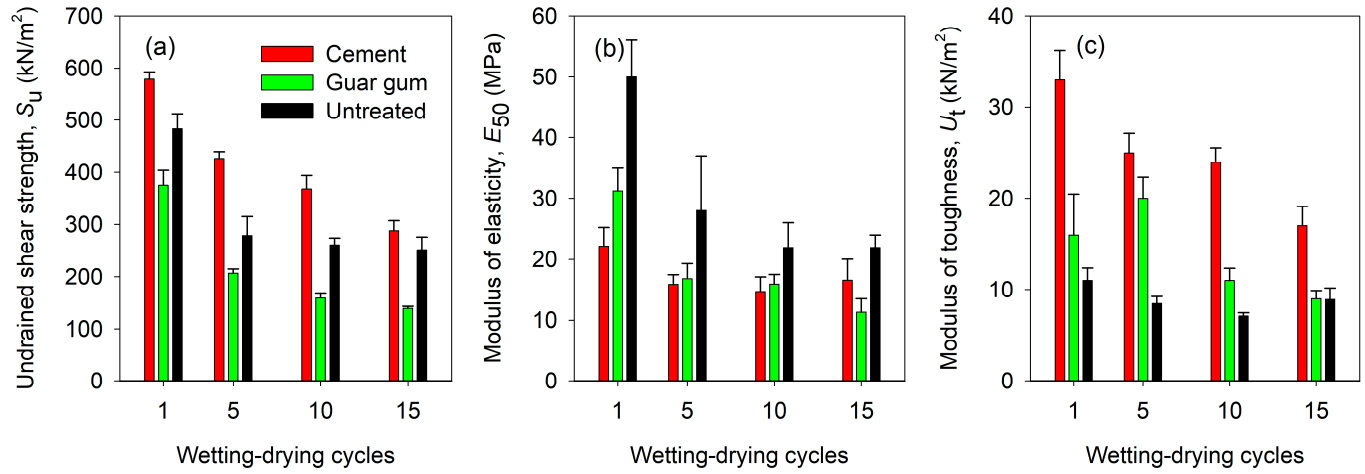

Figure 5. Variation in (**a**) undrained shear strength, (**b**) secant modulus of elasticity, and (**c**) modulus of toughness measured at −1500 kPa matric suction for untreated soil and soil treated with cement and guar gum, subjected to 1, 5, 10, and 15 wetting–drying cycles.

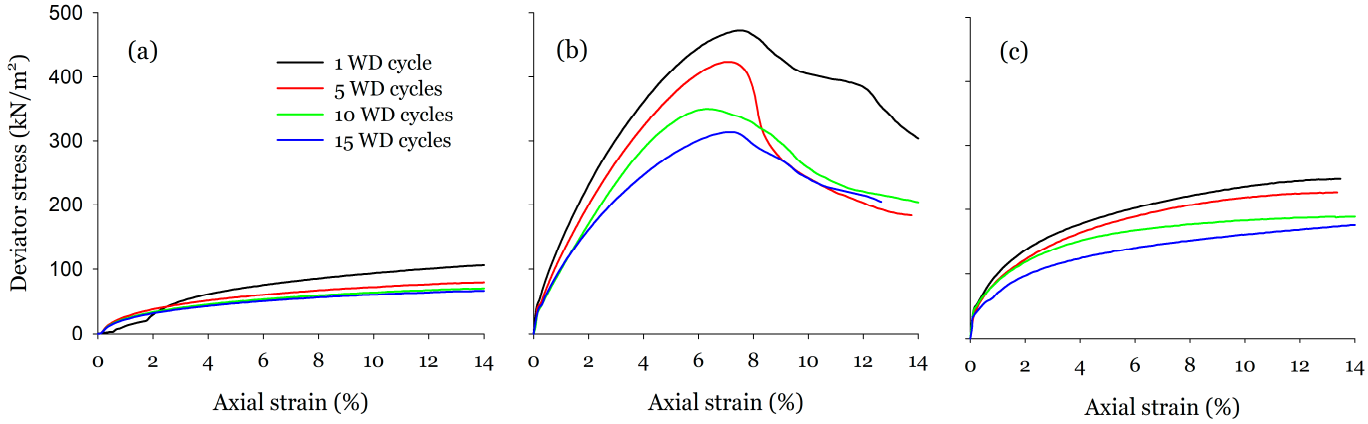

Figure 6. Deviator stress is plotted as a function of axial strain (average for three samples) measured at the matric suction of −33 kPa for (**a**) untreated soil, (**b**) cement-treated soil, and (**c**) guar gum-treated soil for 1, 5, 10, and 15 wetting–drying cycles.

At −33 kPa matric suction, all soil samples exhibited a reduction in undrained shear strength (S_u) compared to those tested at −1500 kPa, primarily due to the increased pore water content diminishing matric suction. The untreated soil demonstrated a progressive

decline in strength with increasing WD cycles, decreasing from 54 kPa after the first cycle to 33 kPa after 15 cycles—a reduction of approximately 39%. Cement-treated soil initially recorded the highest S_u (235 kPa), but this value declined steadily to 156 kPa after 15 cycles (34% reduction), indicating degradation of cementitious bonds due to moisture ingress. Nevertheless, it consistently outperformed the other treatments throughout the WD cycles. Guar gum-treated soil displayed an intermediate response, with S_u decreasing from 124 kPa to 92 kPa (26% reduction), suggesting relatively better resilience against moisture-induced weakening than the untreated soil, albeit inferior to cement treatment in terms of absolute strength (Figure 7a). The variation in the secant modulus of elasticity (E_{50}) with respect to WD cycles mirrored the trends observed in S_u (Figure 7b). Interestingly, the guar gum-treated soil exhibited the highest modulus of toughness (U_t), surpassing both cement-treated and untreated soils (Figure 7c), indicating its superior energy absorption capacity under cyclic moisture fluctuations.

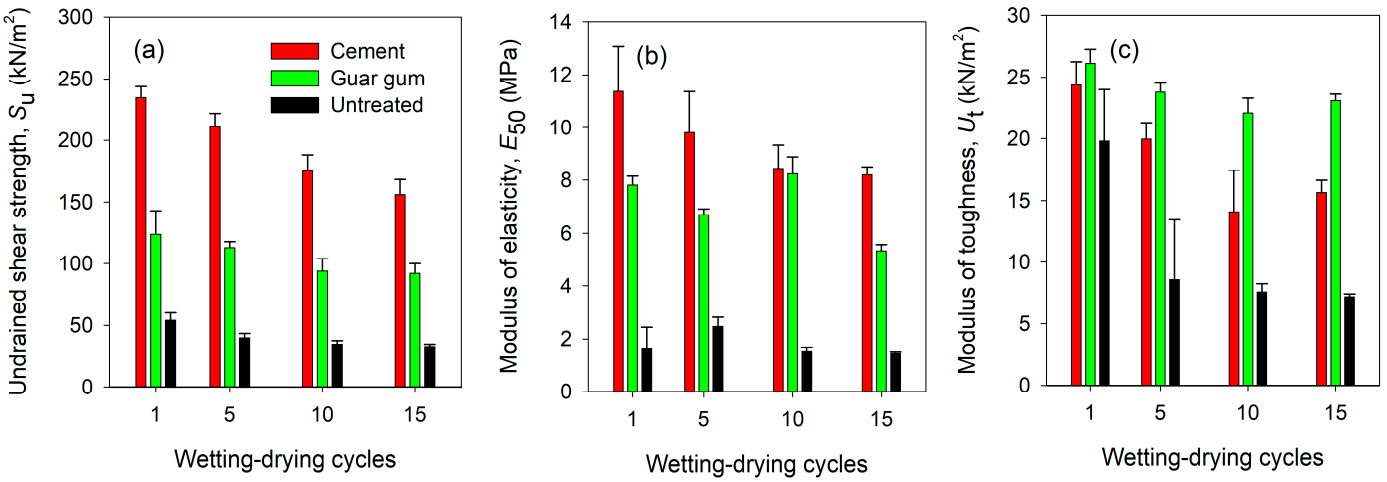

Figure 7. Variation in (**a**) undrained shear strength, (**b**) modulus of elasticity, and (**c**) modulus of toughness measured at −33 kPa matric suction for untreated soil and soil treated with cement and guar gum, subjected to 1, 5, 10, and 15 wetting–drying cycles.

3.4. Stress–Strain Behaviour at Saturation

Undrained triaxial shear strength tests conducted under saturation provided key insights into the long-term mechanical performance of soils stabilised with cement and guar gum, particularly following repeated wetting–drying (WD) cycles. All soil samples displayed strain-hardening behaviour under saturated conditions, except cement-treated samples subjected to one and five WD cycles (Figure 8). The undrained shear strength (S_u) of the untreated soil decreased from 28 kPa after 1 WD cycle to 17 kPa after 15 cycles, representing a 38% reduction in strength. Cement-stabilised samples exhibited a significantly higher initial S_u of 72 kPa after 1 WD cycle; however, this value declined to 27 kPa after 15 cycles (a 62% reduction), likely due to microcracking and calcium leaching. Despite this degradation, the cement-treated soil retained superior strength to the untreated control. Guar gum-stabilised soil demonstrated a S_u of 49 kPa at 1 WD cycle, decreasing moderately to 29 kPa after 15 cycles, amounting to a 40% reduction. It is worth noting that S_u for the guar gum-treated soil under 10 and 15 WD cycles is very similar to that of cement-treated soil (Figure 9a).

Figure 9b presents the secant modulus of elasticity (E_{50}), determined under saturated conditions for untreated, cement-treated, and guar gum-treated soils across 1, 5, 10, and 15 WD cycles. Notably, the highest modulus of toughness (U_t) was recorded for the guar gum-treated samples, followed by cement-treated and untreated soils (Figure 9c),

underscoring the energy absorption capacity and ductility enhancement afforded by the biopolymer treatment.

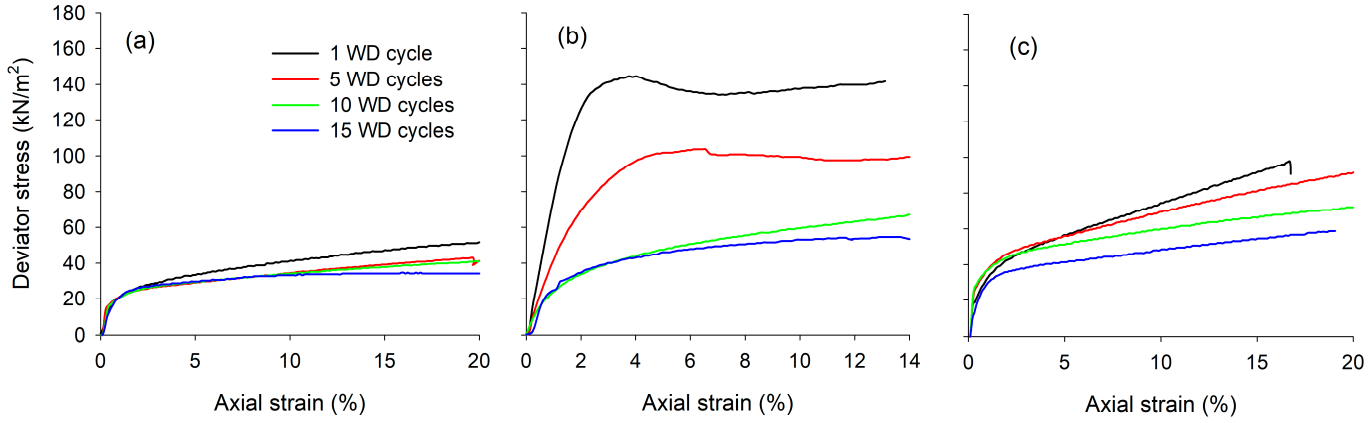

Figure 8. Deviator stress is plotted as a function of axial strain (average for three samples) measured at saturation for (**a**) untreated soil, (**b**) cement-treated soil, and (**c**) guar gum-treated soil for 1, 5, 10, and 15 wetting–drying cycles.

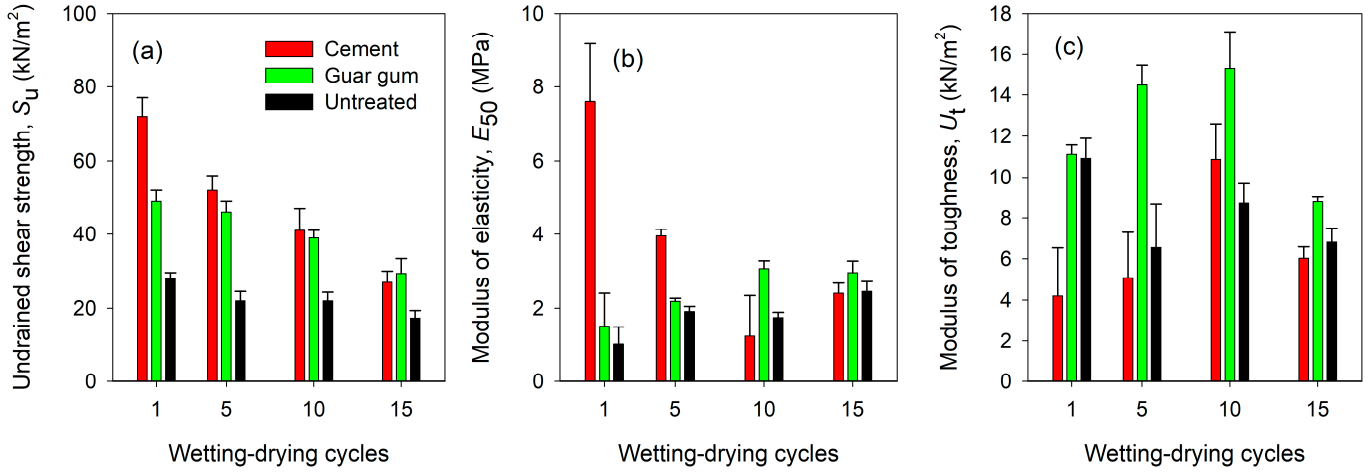

Figure 9. Variation in (**a**) undrained shear strength, (**b**) modulus of elasticity, and (**c**) modulus of toughness measured at saturation for untreated soil and soil treated with cement and guar gum, subjected to 1, 5, 10, and 15 wetting–drying cycles.

3.5. X-Ray CT Visualisation

After one WD cycle (top row, Figure 10), the untreated soil (left) exhibits a heterogeneous microstructure with moderate pore connectivity and visible interparticle spaces, indicating loose particle arrangement. The cement-treated sample (middle) presents a denser and more homogeneous structure, characterised by bright grayscale regions corresponding to cement hydration products and reduced visible pore spaces. Although some macropores are present at the periphery, the guar gum-treated sample (right) also shows improved densification compared to the untreated sample, with relatively uniform grayscale intensity and fewer macropores in the middle, suggesting an early-stage binding effect of guar gum on soil aggregates.

After 10 WD cycles (bottom row), significant structural degradation is observed in the untreated sample, with prominent crack networks and large voids (highlighted by red arrows), especially near the periphery. The cement-treated sample shows minor cracking (red arrows) and limited structural deterioration, maintaining overall integrity due to cementitious bonding. The guar gum-treated specimen exhibits minimal cracking

(red arrow) and preserves a relatively intact microstructure, indicating the biopolymer's resilience against moisture-induced cyclic stresses (Figure 10).

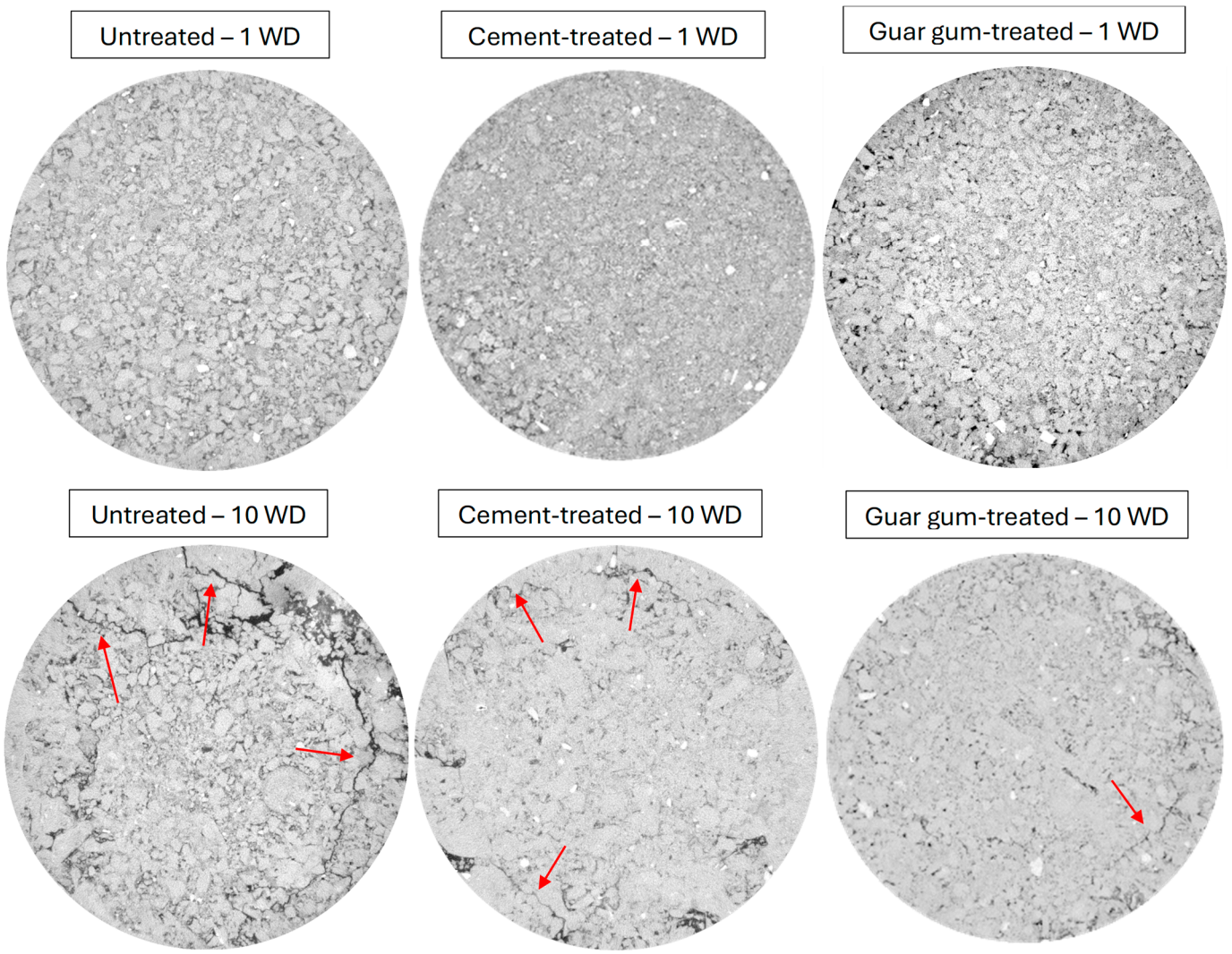

Figure 10. X-ray computed tomography (CT) grayscale images illustrate expansive soil samples' internal microstructural evolution under cyclic wetting–drying (WD) conditions. The images compare untreated, cement-treated, and guar gum-treated samples after 1 and 10 WD cycles. All images represent horizontal cross-sections at mid-height of cylindrical samples, and cracks are marked with red arrows.

These CT images collectively highlight the superior resistance of cement and guar gum treatments in preserving the microstructural stability of expansive soils under repeated environmental loading.

3.6. Cost–Carbon Emission Comparison Analysis

Table 1 presents a comparative analysis of cement and guar gum as soil-stabilising agents, highlighting their economic and environmental implications when used to treat 1 m^3 of soil with a target dry density of 1.6 g/cm^3 (1600 kg/m^3). Cement was applied at a dosage of 6%, corresponding to 96 kg/m^3 of soil, whereas guar gum was used at a lower dosage of 1%, requiring 16 kg/m^3. Despite the higher unit cost of guar gum (GBP 1500/ton) compared to cement (GBP 150/ton), the total material cost for treating 1 m^3 of soil with guar gum (GBP 24) exceeded that of cement (GBP 15), due to the significantly higher price per unit mass [33,34].

Table 1. Cost and CO_2 emission comparison for cement and guar gum to stabilise 1 m^3 of soil.

Material	Target Density of Soil (kg/m^3)	Dosage (%)	Quantity Required for 1 m^3 of Soil (kg)	Cost per Ton (GBP)	Total Cost for 1 m^3 Soil (GBP)	CO_2 Emissions per Ton (ton)	Total CO_2 Emissions for 1 m^3 Soil (kg)
Cement	1.6	6	96	150	15	0.9	86.4
Guar gum		1	16	1500	24	0.1	1.6

Regarding environmental impact, cement production produces substantial CO_2 emissions of 0.9 tons per ton of material, translating to 86.4 kg CO_2 per m^3 of treated soil [35]. In contrast, guar gum exhibits a markedly lower carbon footprint of only 0.1 tons of CO_2 per ton, resulting in a minimal emission of 1.6 kg CO_2 per m^3 of soil [36]. This comparison underscores guar gum's potential as a more environmentally sustainable, albeit costly, alternative to cement for soil improvement applications.

4. Discussion

4.1. Volumetric Response and Moisture Dynamics

The observed volumetric instability in untreated expansive soils subjected to cyclic wetting–drying (WD) aligns well with established behaviours documented in highly plastic clays [5,7]. Notably, the progressive reduction in swelling from approximately 14% to a range of 8–10% over 15 cycles suggests a significant degree of structural degradation and pore collapse, resulting in a densified matrix with diminished water retention capacity. The pronounced shrinkage strains, ranging from −2% to −7%, coupled with observable crack propagation, underscore the potential durability concerns arising from seasonal hydric fluctuations [13].

In contrast, cement-treated soils exhibited a distinctly different behaviour, with swelling strains increasing from 22% to 30% across successive cycles, despite an initial high strength. This behaviour can be attributed to internal structural evolution, characterised by microcracking resulting from repeated moisture ingress and the precipitation of expansive hydration products, such as ettringite, which further promotes volumetric expansion [37]. The increase in saturation moisture content to 43% highlights an increase in macroporosity resulting from the destabilisation of cementitious bonds and the leaching of soluble phases. Notably, the residual swelling appeared to plateau at approximately 15%, indicating the formation of semi-stable matrices capable of retaining volumetric memory through cycles.

Guar gum-treated soils demonstrated volumetric responses similar to untreated soils regarding swelling–shrinkage amplitude; however, they exhibited distinct moisture migration behaviours. The delayed saturation observed in guar gum-treated soils (~6 days compared to 4 days for untreated soils) and the reduced severity of cracks point to the beneficial role of the polysaccharide in enhancing particle bridging and minimising capillary connectivity [38]. This behaviour is consistent with previous studies indicating that biopolymer treatments effectively limit surface evaporation and manage pore pressure buildup, thereby mitigating damage driven by desiccation [27]. While the mechanical improvements were modest, guar gum-treated soils' enhanced integrity and crack resistance underscore their potential to mitigate hydraulic fatigue. This is evident from the X-ray CT grayscale images of soil columns in Figure 10.

4.2. Mechanical Performance Under WD Cycles

At −1500 kPa matric suction, all soils displayed strain-softening behaviour, typical of unsaturated fine-grained soils with apparent cohesion [39]. Cement-treated soils exhibited the highest undrained shear strength (S_u), owing to the formation of calcium silicate hydrates (CSHs) and calcium aluminate hydrates (CAHs), which enhance interparticle

bonding [40]. However, the progressive S_u reduction (579 to 288 kPa from 1 to 15 WD cycles) underscores the vulnerability of cementitious bonds to cyclic moisture intrusion and microstructural fatigue [40–42]. Interestingly, untreated soils maintained higher E_{50} values than treated soils at −1500 kPa matric suction, possibly due to their naturally compacted and stiff state with high matric suction. This is congruent with studies showing suction-induced stiffness dominates compacted unsaturated clays [43]. In contrast, the lower modulus values in treated soils may reflect the presence of hydrated gels and entrapped voids introduced during treatment, contributing to increased deformability. Despite exhibiting lower S_u than untreated soils, guar gum-treated soils maintained a comparatively higher modulus of toughness (U_t). This implies enhanced energy dissipation capacity under monotonic loading—a critical factor in resisting progressive cracking and deformation in cyclic environments [44].

At −33 kPa matric suction, the untreated soil showed the most pronounced reduction in S_u (39%) with WD cycles from 1 to 15, corroborating Shah et al.'s [45] observations of exponential strength loss with WD cycles. Guar gum treatment yielded superior toughness and relatively stable S_u (124 to 92 kPa, ~26% drop), indicating biopolymer-mediated enhanced ductility and pore water buffering. These results agree with Hamza et al. [44], who reported that moisture entrapment within biopolymer films reduces pore pressure gradients and crack propagation.

The saturated state provided a worst-case scenario for long-term treatment efficacy. As expected, all soils showed reduced undrained shear strength (S_u) due to the complete loss of matric suction. In untreated soils, the undrained shear strength decreased from 28 kPa to 17 kPa, marking a substantial 38% reduction over 15 WD cycles. In contrast, samples stabilised with cement experienced even greater degradation, with strength plummeting from 72 kPa to 27 kPa, reflecting an extraordinary 62% decline under the same conditions, indicative of extensive chemical bond degradation with WD cycles. Microcracking and leaching of calcium-based products likely facilitated a reduction in solid-phase continuity [40–42]. Despite this, cement-treated soil maintained the highest absolute strength among all treatments, affirming its structural advantage even under extreme saturation. Guar gum-treated soils demonstrated moderate strength loss (49 to 29 kPa from 1 to 15 WD cycles, ~40% drop) but preserved the highest toughness across all WD cycles. This performance reinforces the notion of guar gum as a ductility enhancer, promoting distributed deformation rather than brittle failure. Its physical–chemical interactions likely form a pseudo-gel matrix that binds particles while allowing limited deformation under stress, thus maintaining post-peak energy absorption capacity [38,44].

In the most adverse conditions tested, the undrained shear strength (S_u) of guar gum-treated samples remained above 29 kPa after 15 wetting–drying (WD) cycles under saturated conditions, outperforming cement-treated samples, which exhibited a comparable S_u of 27 kPa at the same stage. According to Eurocode 7 [46] and prevailing geotechnical design practices, a $S_u \geq 25$ kPa is generally deemed sufficient for lightly loaded structures, such as road subgrades, embankments, and shallow foundations, on soft cohesive soils. Notably, guar gum-treated soils also exhibited the highest modulus of toughness (U_t) across all moisture conditions, indicating superior energy absorption capacity and ductility. These characteristics are particularly advantageous in applications subjected to repeated environmental loading, such as seasonal moisture fluctuations or rainfall cycles. The elevated toughness values suggest enhanced resistance to cracking and a reduced likelihood of brittle failure, aligning with long-term performance expectations for resilient and sustainable infrastructure [47,48]. Moreover, X-ray computed tomography (CT) imaging revealed that guar gum-treated samples maintained superior microstructural integrity after 10 wetting–drying (WD) cycles, displaying significantly fewer and narrower cracks than

both untreated and cement-stabilised counterparts. This evidence underscores the effectiveness of biopolymer stabilisation in enhancing resistance to moisture-induced degradation, thereby supporting its suitability for geotechnical applications demanding long-term mechanical and volumetric stability. To build upon these findings, future research should employ advanced quantitative image-processing techniques to systematically evaluate pore structure parameters and crack density across untreated, cement-treated, and guar gum-treated soils subjected to repeated WD cycling.

4.3. Sustainability Assessment

The sustainability analysis reveals a stark trade-off between mechanical performance and environmental impact. Although cement remains more cost-effective (GBP 15/m^3 vs. GBP 24/m^3 for guar gum), its environmental burden (86.4 kg CO_2/m^3) is nearly 54 times greater than that of guar gum (1.6 kg CO_2/m^3), aligning with global concerns regarding cement's embodied carbon. Costs may be reduced by using industrial-grade or partially refined guar gum, which is substantially cheaper than food-grade powder. Additionally, blending guar gum with other low-cost additives, such as fly ash or lime, can enhance performance while further reducing total costs. While guar gum incurs higher upfront costs, its potential for long-term durability under cyclic environmental loading and its ultra-low carbon footprint render it a viable alternative for green infrastructure applications. This may qualify guar gum for use in public works funded under sustainability targets, helping to offset initial material costs [49–51].

4.4. Biodegradation Risks and Matrix Influence in Guar Gum-Stabilised Soils

Though the guar gum is proven to be a viable alternative for soil stabilisation under cyclic environmental loading, concerns remain about its long-term stability under subsurface conditions, particularly regarding biodegradation by indigenous soil microorganisms. Microbial degradation poses a potential risk to the durability and performance of guar gum-treated soils over extended periods [52]. Recent studies indicate that the risk of biodegradation can be substantially reduced when guar gum is incorporated within low-permeability clay matrices. These dense clay environments act as physical and biochemical barriers that limit microbial access to guar gum molecules, thereby reducing microbial activity and slowing degradation [53]. For example, compacted clay soils create microenvironments with limited oxygen diffusion and nutrient availability, which suppress microbes' abundance and metabolic function capable of degrading biopolymers like guar gum. In particular, saturated or anaerobic conditions common in guar gum-stabilised clay soils further restrict microbial degradation processes, potentially extending the functional lifespan of the stabilisation treatment [54]. However, the extent of this protective effect depends heavily on site-specific factors, including clay mineralogy, pore water chemistry, and redox potential, all of which influence microbial populations and activity. Therefore, while guar gum stabilisation shows promise for durable soil improvement, further research, especially long-term field studies, is necessary to better understand how biodegradation progresses under varying geochemical and hydrological scenarios. Such investigations will help validate laboratory results and clarify guar gum's practical longevity and effectiveness as a sustainable soil stabiliser [52].

5. Conclusions

The results of this study revealed distinct moisture and mechanical responses of expansive soils treated with cement and guar gum under cyclic wetting–drying (WD) conditions. Untreated soils exhibited high initial swelling (~14%) and shrinkage (−2% to −7%), which diminished over cycles due to structural degradation. Cement-treated soils

showed increasing swelling (22% to 30%) with higher saturation moisture contents (up to 43%), attributed to microcracking and expansive hydration products. Despite strength gains, post-drying residual swelling plateaued at ~15%. Guar gum-treated samples had similar volumetric strains to untreated soils but demonstrated improved crack resistance and delayed saturation due to reduced water infiltration and better structural cohesion.

Mechanically, all soils showed strain-softening at −1500 kPa suction, with cement-treated soils achieving the highest undrained shear strength (S_u), though degrading from 579 to 288 kPa over 15 cycles. Guar gum-treated soils exhibited lower S_u but retained higher toughness, reflecting superior energy absorption. At −33 kPa suction, cement again provided the highest S_u, but guar gum-treated soils retained strength more effectively (26% reduction vs. 34% for cement) and achieved the highest toughness, highlighting their ductility. Under saturation, all soils showed strain-hardening, with S_u for cement and guar gum-treated samples being comparable, yet guar gum-treated soils maintained the highest toughness. These benefits were attributed to the biopolymer's pore-blocking effects and cohesive gel network.

A preliminary cost–carbon assessment demonstrated that guar gum, despite its higher unit cost (GBP 24/m^3 compared to GBP 15/m^3 for cement), offers a markedly lower carbon footprint, with CO_2 emissions of only 1.6 kg/m^3 versus 86.4 kg/m^3 for cement. This substantial reduction in embodied carbon underscores the environmental advantages of guar gum as a sustainable binder. Beyond its ecological benefits, guar gum-treated soils exhibited improved ductility, superior crack resistance, and greater long-term performance under cyclic environmental loading—characteristics essential for stabilising expansive soils. These results position guar gum as a technically viable and environmentally favourable alternative to conventional cementitious stabilisers. However, further investigations, particularly extended in situ studies, are warranted to establish its field applicability and long-term durability fully. Such research should focus on the influence of varying geochemical and hydrological conditions on the biodegradation behaviour of guar gum, thereby bridging the gap between laboratory observations and real-world performance.

Author Contributions: Conceptualisation, M.N. and K.S.T.; methodology, M.N., S.S.A.S. and K.S.T.; formal analysis, M.N., S.S.A.S. and K.S.T.; investigation, S.S.A.S. and K.S.T.; writing—original draft preparation, M.N. and K.S.T.; writing—review and editing, M.N., S.S.A.S. and K.S.T.; visualisation, K.S.T.; supervision, M.N.; project administration, M.N.; funding acquisition, M.N. and K.S.T. All authors have read and agreed to the published version of the manuscript.

Funding: This research was funded by the PhD Vice Chancellor Scholarship for Kanishka S. Turrakheil at the University of West London.

Institutional Review Board Statement: Not applicable.

Informed Consent Statement: Not applicable.

Data Availability Statement: Due to privacy, the data presented in this study are available upon request from the corresponding author.

Acknowledgments: We thank the anonymous reviewers for their time and comments. The National Research Facility for Lab X-Ray CT(NXCT)at the μ-VIS X-ray Imaging Centre, University of Southampton, supported the X-ray computed tomography scanning through EPSRC grant EP/T02593X/1.

Conflicts of Interest: The authors declare no conflicts of interest.

Appendix A

Table A1. A complete set of measured data in this study.

Treatment	Matric Suction (kPa)	WD Cycles (No.)	Moisture Content (%)	Undrained Shear Strength, S_u (kPa)	Secant Modulus of Elasticity, E_{50} (MPa)	Modulus of Toughness, U_t (kPa)
Untreated	−1500	1	12 ± 0.5	483 ± 29	50.2 ± 6.1	11 ± 1.4
		5	12 ± 0.43	279 ±36	28.4 ± 9.3	8.5 ± 0.8
		10	13 ± 0.68	261 ± 13	22.3 ± 4.2	7.1 ± 0.4
		15	12 ± 0.29	252 ± 24	22.1 ± 1.8	8.9 ± 1.3
	−33	1	19 ± 0.79	54 ± 3	1.6 ± 0.8	19.8 ± 4.2
		5	17 ± 0.83	40 ± 4	2.5 ± 0.3	8.6 ± 4.9
		10	17 ± 0.48	35 ± 3	1.5 ± 0.2	7.6 ± 0.7
		15	16 ± 0.39	33 ± 2	1.4 ± 0.1	7.2 ± 0.2
	0	1	26 ± 2.43	28 ± 2	1.0 ± 0.4	10.9 ± 0.9
		5	22 ± 1.21	22 ± 3	1.9 ± 0.1	6.6 ± 2.1
		10	21 ± 0.95	22 ± 2	1.8 ± 0.2	8.7 ± 0.9
		15	21 ± 1.01	17 ± 2	2.5 ± 0.3	6.8 ± 0.7
Cement-treated	−1500	1	14 ± 0.98	579 ± 14	22.3 ± 3.4	33.3 ± 3.2
		5	15 ± 1.18	427 ± 13	16.7 ± 2.3	25.9 ± 2.1
		10	12 ± 0.28	368 ± 16	15.2 ± 1.9	24.2 ± 1.6
		15	14 ± 1.38	288 ± 19	17.1 ± 3.6	17.3 ± 2.1
	−33	1	24 ± 0.95	235 ± 9	11.4 ± 1.7	24.4 ± 1.9
		5	24 ± 0.81	211 ± 11	9.8 ± 1.6	19.9 ± 1.3
		10	22 ±0.78	175 ± 13	8.4 ± 0.9	14.1 ± 3.3
		15	24 ± 0.69	156 ± 12	8.2 ± 0.3	15.6 ± 0.9
	0	1	32 ± 1.31	72 ± 5	7.6 ± 1.6	4.2 ± 2.3
		5	34 ± 1.34	52 ± 4	4.0 ± 0.2	5.1 ± 0.2
		10	34 ± 1.52	41 ± 6	1.2 ± 1.1	10.9 ± 1.7
		15	33 ± 1.23	27 ± 3	2.4 ± 0.3	6.0 ± 0.6
Guar gum-treated	−1500	1	12 ± 0.36	375 ± 29	31.2 ± 3.8	16.3 ± 4.5
		5	13 ± 0.44	207 ± 8	17.9 ± 3.4	20.1 ± 2.3
		10	11 ±0.23	159 ± 5	15.5 ± 2.1	11.4 ± 1.3
		15	12 ± 0.09	139 ± 4	11.7 ± 2.2	9.4 ± 0.9
	−33	1	17 ± 0.56	124 ± 19	7.8 ± 0.3	26.1 ± 1.1
		5	16 ± 0.89	113 ± 5	6.7 ± 0.2	23.8 ± 0.7
		10	16 ± 0.49	94 ± 10	8.2 ± 0.2	22.1 ± 1.2
		15	17 ± 0.94	92 ± 8	5.3 ± 0.2	23.1 ± 0.5
	0	1	24 ± 1.89	49 ± 3	1.5 ± 0.9	11.1 ± 0.5
		5	22 ± 0.67	46 ± 3	2.2 ± 0.1	14.5 ± 0.9
		10	22 ± 0.38	39 ± 2	3.1 ± 0.2	15.3 ± 1.8
		15	22 ± 0.39	29 ± 4	2.6 ± 0.3	8.8 ± 0.2

References

1. Intergovernmental Panel on Climate Change (IPCC). *Climate Change 2021: The Physical Science Basis*; Cambridge University Press: Cambridge, UK, 2021.
2. Shah, S.S.A.; Turrakheil, K.S.; Naveed, M. Impact of wetting and drying cycles on the hydromechanical properties of soil and implications on slope stability. *Atmosphere* **2024**, *15*, 1368. [CrossRef]
3. Ng, C.W.W.; Leung, A.K.; Woon, K.H. Effects of soil density on grass-induced suction distributions in compacted soil subjected to rainfall. *Can. Geotech. J.* **2014**, *51*, 311–321. [CrossRef]
4. Goh, S.G.; Rahardjo, H.; Leong, E.C. Shear strength of unsaturated soils under multiple drying–wetting cycles. *J. Geotech. Geoenviron. Eng.* **2014**, *140*. [CrossRef]
5. Tripathy, S.; Subba Rao, K.S.; Fredlund, D.G. Water content–void ratio swell–shrink paths of compacted expansive soils. *Can. Geotech. J.* **2002**, *39*, 938–959. [CrossRef]
6. Yesiller, N.; Miller, C.J.; Inci, G.; Yaldo, K. Desiccation and cracking behavior of three compacted landfill liner soils. *Eng. Geol.* **2000**, *57*, 105–121. [CrossRef]

7. Turrakheil, K.S.; Shah, S.S.A.; Naveed, M. Evolution of soil pore structure and shear strength deterioration of compacted soil under controlled wetting and drying cycles. *Atmosphere* **2024**, *15*, 843. [CrossRef]
8. Narsilio, G.A.; Santamarina, J.C.; Altschaeffl, A.G. Effects of wetting-drying cycles and desiccation cracks on mechanical behaviour of an unsaturated soil. *Catena* **2020**, *194*, 104721. [CrossRef]
9. Albrecht, B.A.; Benson, C.H. Effect of desiccation on compacted natural clays. *J. Geotech. Geoenviron. Eng.* **2001**, *127*, 67–75. [CrossRef]
10. Cui, Y.J.; Tang, A.M.; Mantho, A.T.; De Laure, E. Monitoring field soil suction using miniature tensiometers. *Geotech. Test. J.* **2008**, *31*, 95–100. [CrossRef]
11. Simona, S.; Barnichon, J.D.; Cui, Y.J.; Tang, A.M.; Delage, P. Microstructure and anisotropic swelling behaviour of compacted bentonite/sand mixture. *J. Rock Mech. Geotech. Eng.* **2014**, *6*, 126–132. [CrossRef]
12. Mitchell, J.K.; Soga, K. *Fundamentals of Soil Behaviour*, 3rd ed.; Wiley: Hoboken, NJ, USA, 2005.
13. Chen, R.; Ng, C.W.W. Impact of wetting–drying cycles on hydro-mechanical behavior of an unsaturated compacted clay. *Appl. Clay Sci.* **2013**, *86*, 38–46. [CrossRef]
14. Nabil, M.; Mustapha, A.; Rios, S. Impact of wetting–drying cycles on the mechanical properties of lime-stabilized soils. *Int. J. Pavement Res. Technol.* **2020**, *13*, 83–92. [CrossRef]
15. Wassermann, A.; Abdallah, A.; Cuisinier, O. Impact of wetting and drying cycles on the mechanical behaviour of a cement-treated soil. *Transp. Geotech.* **2022**, *36*, 100804. [CrossRef]
16. Consoli, N.C.; Prietto, P.D.M.; Ulbrich, L.A. Influence of fiber and cement addition on behavior of sandy soil. *J. Geotech. Geoenviron. Eng.* **1998**, *124*, 1211–1214. [CrossRef]
17. Hopkins, T.C.; Hunsucker, D.Q.; Beckham, T. Long-term performance of flexible pavements located on cement-treated soils. *Transp. Res. Rec.* **1994**, *1440*, 20–28.
18. Lv, S.; Xia, C.; Liu, H.; You, L.; Qu, F.; Zhong, W.; Yang, Y.; Washko, S. Strength and fatigue performance for cement-treated aggregate base materials. *Int. J. Pavement Eng.* **2019**, *22*, 690–699. [CrossRef]
19. Roberts, J.D. *Performance of Cement-Modified Soils: A Follow-Up Report*; Federal Highway Administration: Washington, DC, USA, 1986.
20. Niu, W.; Guo, B.; Li, K.; Ren, Z.; Zheng, Y.; Liu, J.; Lin, H.; Men, X. Cementitious material-based stabilization of soft soils by stabilizer. *Constr. Build. Mater.* **2024**, *425*, 136046. [CrossRef]
21. Dai, D.; Peng, J.; Wei, R.; Li, L.; Lin, H. Improvement in dynamic behaviors of cement-stabilized soil by super-absorbent-polymer under cyclic loading. *Soil Dyn. Earthq. Eng.* **2022**, *163*, 107554. [CrossRef]
22. Azimi, M.; Soltani, A.; Mirzababaei, M.; Jaksa, M.B.; Ashwath, N. Biopolymer stabilization of clayey soil. *J. Rock Mech. Geotech. Eng.* **2024**, *16*, 2801–2812. [CrossRef]
23. Bagriacik, B.; Ok, B.; Kahiyah, M.T.M.A. An experimental study on improvement of cohesive soil with eco-friendly guar gum. *Soils Rocks* **2021**, *44*, e2021060020. [CrossRef]
24. Banne, S.P.; Kulkarni, S.; Baldovino, J.A. Effect of guar gum content on the mechanical properties of laterite soil for subgrade soil application. *Polymers* **2024**, *16*, 2202. [CrossRef]
25. Keshav, N.; Prabhu, A.; Kattimani, A.; Dharwad, A.; Kallatti, C.; Mahalank, S. Enhancing the properties of expansive soil using biopolymers—Xanthan gum and guar gum. In Proceedings of the Indian Geotechnical Conference 2019, Surat, India, 19–21 December 2019; Springer: Singapore, 2021; Volume 138, pp. 121–131. [CrossRef]
26. Sujatha, E.R.; Saisree, S. Geotechnical behaviour of guar gum-treated soil. *Soils Found.* **2019**, *59*, 2155–2166. [CrossRef]
27. Firoozi, A.A.; Olgun, C.G.; Baghini, M.S. Fundamentals of soil stabilization. *Int. J. Geo-Eng.* **2017**, *8*, 26. [CrossRef]
28. Chang, I.; Lee, M.; Tran, A.T.P.; Lee, S.; Kwon, Y.-M.; Im, J.; Cho, G.-C. Review on biopolymer-based soil treatment (BPST) technology in geotechnical engineering practices. *Transp. Geotech.* **2020**, *24*, 100385. [CrossRef]
29. *BS 1377-1:2016*; Methods of Test for Soils for Civil Engineering Purposes—Part 1: General Requirements and Sample Preparation. British Standards Institution (BSI): London, UK, 2016.
30. *BS 1377-7:1990*; Methods of Test for Soils for Civil Engineering Purposes—Part 7: Shear Strength Tests (Total Stress). British Standards Institution (BSI): London, UK, 1990.
31. Rasband, W. ImageJ, *version 1.54h*; U.S. National Institutes of Health: Bethesda, MD, USA, 2023.
32. Subramani, A.K.; Ramani, S.E.; Selvasembian, R. Understanding the microstructure, mineralogical and adsorption characteristics of guar gum blended soil as a liner material. *Environ. Monit. Assess.* **2021**, *193*, 855. [CrossRef]
33. IndexBox. Cement Price in the United Kingdom. 2022. Available online: https://www.indexbox.io/search/cement-price-in-the-united-kingdom/ (accessed on 12 June 2025).
34. Agriwatch. Guar Gum Export Price Analysis. May 2024. Available online: https://www.agriwatch.com/market-report/guar-gum (accessed on 12 June 2025).
35. International Energy Agency (IEA). *Cement Production and CO_2 Emissions: Global Trends and Outlooks*; IEA: Paris, France, 2021; Available online: https://www.iea.org/reports/cement (accessed on 12 June 2025).

36. Kumar, M.A.; Moghal, A.A.B.; Vydehi, K.V.; Almajed, A. Embodied energy in the production of guar and xanthan biopolymers and their cross-linking effect in enhancing the geotechnical properties of cohesive soil. *Buildings* **2023**, *13*, 2304. [CrossRef]
37. Cojean, R. Review of: Al-Rawas, A.A.; Goosen, M.F.A. (Eds.): Expansive Soils: Recent Advances in Characterization and Treatment. *Bull. Eng. Geol. Environ.* **2007**, *66*, 505. [CrossRef]
38. Acharya, R.; Pedarla, A.; Bheemasetti, T.V.; Puppala, A. Assessment of guar gum biopolymer treatment toward mitigation of desiccation cracking on slopes built with expansive soils. *Transp. Res. Rec.* **2019**, *2657*, 78–88. [CrossRef]
39. Rasul, J.M.; Ghataora, G.S.; Burrow, M.P.N. The effect of wetting and drying on the performance of stabilized subgrade soils. *Transp. Geotech.* **2018**, *14*, 1–7. [CrossRef]
40. Horpibulsuk, S.; Rachan, R.; Chindaprasirt, P. Analysis of strength development in cement-stabilized silty clay from microstructural considerations. *Constr. Build. Mater.* **2010**, *24*, 2011–2021. [CrossRef]
41. Cuisinier, O.; Masrouri, F.; Mehenni, A. Alteration of the hydromechanical performances of a stabilized compacted soil exposed to successive wetting–drying cycles. *J. Mater. Civ. Eng.* **2020**, *32*, 04020052. [CrossRef]
42. Estabragh, A.R.; Pereshkafti, M.R.S.; Parsaei, B.; Javadi, A.A. Stabilised expansive soil behaviour during wetting and drying. *Int. J. Pavement Eng.* **2013**, *14*, 418–427. [CrossRef]
43. Ng, C.W.W.; Menzies, B.K. *Advanced Unsaturated Soil Mechanics and Engineering*; Taylor & Francis: London, UK, 2007.
44. Hamza, M.; Nie, Z.; Aziz, M.; Ijaz, N.; Fang, C.; Ghani, M.U.; Ijaz, Z.; Noshin, S.; Salman, M. Geotechnical properties of problematic expansive subgrade stabilized with guar gum biopolymer. *Clean Technol. Environ. Policy* **2023**, *25*, 1699–1719. [CrossRef]
45. Shah, S.N.; Ali, S.A.; Khan, A. Impact of wetting–drying cycles on the mechanical behavior of expansive soils. *Int. J. Geotech. Eng.* **2024**, *18*, 123–134.
46. *EN 1997-1*; Eurocode 7—Geotechnical Design—Part 1: General Rules. CEN: Brussels, Belgium, 2004.
47. Liu, Y.; Ni, J.; Gu, J.; Liu, S.; Huang, Y.; Sadeghi, H. Influence of biopolymer–vegetation interaction on soil hydro-mechanical properties under climate change: A review. *Sci. Total Environ.* **2024**, *954*, 176535. [CrossRef]
48. Reddy, K.R.; Janga, J.K.; Kumar, G. Sustainability and resilience: A new paradigm in geotechnical and geoenvironmental engineering. *Indian Geotech. J.* **2024**. [CrossRef]
49. Scrivener, K.L.; John, V.M.; Gartner, E.M. Eco-efficient cements: Potential economically viable solutions for a low-CO_2 cement-based materials industry. *Cem. Concr. Res.* **2018**, *114*, 2–26. [CrossRef]
50. Abu Dabous, S.; Zeiada, W.; Zayed, T.; Al-Ruzouq, R. Sustainability-informed multi-criteria decision support framework for ranking and prioritization of pavement sections. *J. Clean. Prod.* **2020**, *244*, 118755. [CrossRef]
51. Raj, N.; Selvakumar, S.; Soundara, B.; Kulanthaivel, P. Sustainable utilization of biopolymers as green adhesive in soil improvement: A review. *Environ. Sci. Pollut. Res.* **2023**, *30*, 118117–118132. [CrossRef]
52. Fatehi, H.; Ong, D.E.L.; Yu, J.; Chang, I. Biopolymers as green binders for soil improvement in geotechnical applications: A review. *Geosciences* **2021**, *11*, 291. [CrossRef]
53. Awasthi, S.K.; Kumar, M.; Kumar, V.; Sarsaiya, S.; Anerao, P.; Ghosh, P.; Singh, L.; Liu, H.; Zhang, Z.; Awasthi, M.K. Comprehensive review on recent advancements in biodegradation and sustainable management of biopolymers. *Environ. Pollut.* **2022**, *307*, 119600. [CrossRef] [PubMed]
54. Kögel-Knabner, I.; Amelung, W.; Cao, Z.; Fiedler, S.; Frenzel, P.; Jahn, R.; Kalbitz, K.; Kölbl, A.; Schloter, M. Biogeochemistry of paddy soils. *Geoderma* **2010**, *157*, 1–14. [CrossRef]